All-solid-state electrochromic devices based on $WO_3\|NiO$ films: material developments and future applications

Ding Zhou[1], Dong Xie[1], Xinhui Xia[1,2], Xiuli Wang[1,2], Changdong Gu[1,2] & Jiangping Tu[1,2*]

[1]State Key Laboratory of Silicon Materials, Key Laboratory of Advanced Materials and Applications for Batteries of Zhejiang Province and School of Materials Science and Engineering, Zhejiang University, Hangzhou 310027, China
[2]Cyrus Tang Center for Sensor Materials and Applications, Zhejiang University, Hangzhou 310027, China

Electrochromism refers to the persistent and reversible change of optical properties by an applied voltage pulse. Electrochromic (EC) devices have been extensively studied because of their commercial applications in smart windows of green buildings, display devices and thermal control of equipments. In this review, a basic EC device design is presented based on useful oxides and solid-state electrolytes. We focus on the state-of-the-art research activities related to the structures of tungsten oxide (WO_3) and nickel oxide (NiO), summarizing the strategies to improve their EC performances and further applications of devices.

electrochromic devices, tungsten oxide, nickel oxide, solid-state electrolyte, electrochromism

1   Introduction

Electrochromic (EC) devices are able to control the throughput of visible light and solar radiation into buildings and control energy efficiency by modulating optical transmittance. EC devices are widely studied because of their applications in smart windows of green buildings, full-angle information displays, controlled reflectance mirrors and thermal control of satellites [1–5]. Electrochromism refers to the phenomenon that the optical properties can be switched reversibly and persistently in materials induced upon a small external voltage [6,7]. Two examples of multi-pane installations in which some panes are in their fully colored states and others are bleached are shown in Figure 1.

The study of electrochromism has a long history since the researchers discovered optical changes induced by electricity. Electrically induced color changes in thin films of tungsten oxide immersed in sulfuric acid were given a vivid description in an internal document at Balzers AG in Liechtenstein in 1953 [6,8]. Theoretical considerations suggested that the absorption and emission spectra of certain dyes might shift for hundreds of angstroms upon application of a strong electric field, which was first called "electrochromisim" in 1961 by Platt [9]. Later work by Deb at the American Cyanamide Corporation during the 1960s led to analogous results for WO_3 films, which were first published in seminal papers on electrophotography in 1969 [10] and on basic properties of such films in 1973 [11]. This early history has been authoritatively discussed much later [12]. The principle of a new EC display based on oxidation-reduction reaction of an organic compound of the viologen family was described by Schoot *et al*. [13] in 1973, making the electrochromism into a new developing area. Two monographs [6,14] in 1995 focused largely on solid-state devices. More

---

*Corresponding author (email: tujp@zju.edu.cn or tujplab@zju.edu.cn)

Figure 1 Two examples of multi-panes of EC smart windows [8]. (a) An application of EC smart windows produced by Sage Electrochromics in an office at the Lawrence Berkelecy National Laboratory, USA; (b) an application of EC smart windows produced by ChromoGenics AB in the company's premises in Uppsala, Sweden (color online).

recent reviews introduced more [15–17] or less [18] details. In 2000, Granqvist [17] listed a total review of tungsten oxide films from 1993 to 1998. It seems possible that large-scale printable EC materials could make device cheap and flexible in the future. But this still remains to be studied.

Though the electrochromism technology has been developed for more than half a century, some problems, such as limited color change, slow switching speed, poor cycling stability and lack of device assembly technology, still limit its commercialization and need to be solved by minor physical or chemical modification.

In this review, we discuss the basic EC device designs, useful oxide materials (tungsten oxide/nickel oxide), solid-state electrolyte and their further applications. In addition, we also focus on the state-of-the-art researches of tungsten oxide (WO_3) and nickel oxide (NiO), including their structure and the strategies to improve their EC performances.

2   A typical EC device design

Figure 2 sketches a standard EC device, which is also called five-layer "battery-type" design [3,6]. It has five superimposed thin layers placed between two transparent substrates. The optical function usually originates in the EC films, which change their optical transmittance (reflectance or absorption) when ions are inserted or extracted. The ion

storage films may be a non-coloring redox material, which is referred to as the "counter electrode". The ion storage films can also be EC films, which are called "complementary-type" device. The electrolyte in this diagram may be metallic oxide or a polymer gel in which the salt "MX" is dissolved. MX can be $LiClO_4$ or H_2SO_4 or other salts. These five films are described below.

2.1   Electrochromic mechanism

As shown in the schematic illustration of a transmission type EC device (Figure 2), a typical EC device has an EC layer, an ion-storage layer, an electrolyte layer and two transparent conductive layers. An EC device enables redox electrochemical reactions in it. Taken the typical anodic coloration material WO_3 as a sample, when an anodic pulse of current is applied on the EC layer, cations (H^+, Li^+) inserted into WO_3, which changes the valence state of W atoms and therefore shows blue color. Meanwhile, cations are supplied by the ion storage layer and pass through the electrolyte layer. For electric equilibrium, electrons are inserted into WO_3 from the transparent conductive layer through out circuit.

2.2   Electrochromic films

EC films are grown uniformly on the transparent conducting substrate in order to achieve an even current distribution and thereby reasonably fast and uniform coloring/bleaching [8]. EC films are the key to exhibit color change by an electrochemical reaction. They should have large optical modulation, high coloration efficiency (CE) and cyclic durability. Additionally, EC films also have high electronic conductivity and ionic conductivity to ensure a relatively shorter switching time. In this review, we choose WO_3 as EC materials (Section 3.1).

2.3   Ion storage films

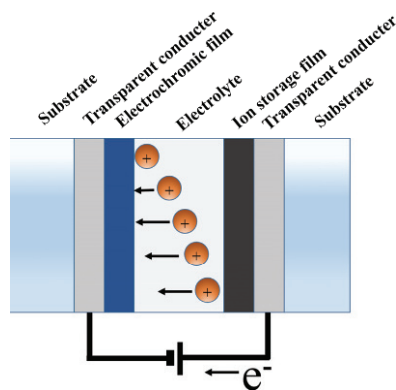Ion storage films are mainly used for storing ions and

Figure 2 A typical EC device design. Arrows indicate the movement of ions in an applied electric field (color online).

keeping electric charge balanced. These films can also be EC films, which have the color overlay or complementary effect. Ion storage films possess high electronic conductivity and ionic conductivity to ensure a relatively shorter switching time. In this review, we choose NiO as ion storage films (Section 3.2).

2.4   Electrolytes

The electrolyte in the center of the EC device must have high ion conductivity, very low electrical conductivity and high durability under solar irradiation. Liquid electrolytes are easy to use widely available and the most durable so far. However, liquid electrolytes could be messy during handling device fabrication and leakage. Though the sealant in the highly successful Gentex car mirror system has an excellent non-leakage record [19]. Solid electrolytes should become the future trend of EC device' development. Solid electrolytes are usually a solid inorganic salt or polymers containing occluded salt. The polymers act as solvent and are often in gel form. In the five-layer "battery-type" design, the electrolyte must be transparent with no color change when EC device works.

2.5   Transparent conductors and substrates

The transparent conductors are pure electron conductors, which are usually tin-doped indium oxide (ITO) or fluorine doped tin oxide (FTO). The transparent conductors have significant effect on EC devices. These materials usually are grown uniformly on the substrates as thin films and have high transmittance, electronic conductivity and good acid and alkali resistance. The transparent substrates for EC devices are often glass, but polymers such as polyethylene terephthalate (PET) or polycarbonate (PC) can also be used.

2.6   Synthesis of the all-solid-state electrochromic devices

The fabrication of an all-solid-state EC device can be divided into typical routs depending on the type of electrolyte used in the device: for the gel polymer electrolyte (GPE, noted as quasi solid state electrolyte), an EC device can be fabricated by sealing GPE between EC layer and ion-storage layer; for fast ionic conductor (ceramic solid electrolyte), an EC device should be fabricated layer-by-layer using vacuum deposition technique.

3   Overview of inorganic EC materials and electrolytes

Generally, there are two types of EC metal oxides, which are called "cathode" (coloring under ion insertion) and "anode" (coloring under ion extraction). Metals that are

capable of forming oxide of these two types are shown in Figure 3. In recent studies, metal oxides based on vanadium are regarded as "hybrid" [6]. In this review, the standard EC device is consist of two EC films, which is obviously advantageous to combine one "cathodic" oxide (such as WO_3 [20–22], MoO_3 [23,24] or TiO_2 [25–27]) and one "anodic" oxide (such as NiO [28–30] or Co_3O_4 [31,32]). The electrolytes are between "cathode" and "anode", which are of primary importance for EC devices. Shuttling ions between these two thin films make them both colored and bleached, which is sometimes called a "battery-type" design [33]. However, electrolytes are generally proprietary for EC devices, and very little is known about those used in commercial applications.

3.1   Tungsten oxide

To date, WO_3 has been considered as one of the most promising "cathodic" oxide due to its tender color change and large color contrast as well as facile synthesis [20,34,35]. The general approaches of fabricating WO_3 films are shown in Table 1. Albeit these advantages, the EC performance of dense WO_3 film is still not satisfactory because of its low diffusion coefficient and long diffusion length for ion insertion [36,37].

The EC performance of WO_3 strongly depends on its crystal structure and architecture [38]. Hence, metal doping, nanostructure and composite design have been proven as effective strategies for improving the EC performance of WO_3 film.

3.1.1   Nanostructures

Nanostructures, including nanowires, nanorods and nanosheets, have been proven to be effective for fabricating high-performance EC films since this architecture can provide fast ion/electron transfer path and large active surface, leading to enhanced optical modulation and fast response time. Typically, one-dimensional (1D) nanowire is desired for EC materials because of its higher specific surface area and porosity.

Figure 3   Periodic table of the elements (the shaded boxes refer to the transition metals whose oxides have well-documented cathodic and anodic electrochromism) [8].

Table 1   General approaches of fabricating WO$_3$ films

Number	Morphology	Method	Reference
1	thin film	magnetron sputtering	[39]
2	thin film	pulsed laser deposition	[40]
3	dense film	electrodeposition	[41]
4	macroporous film	anodic oxidation	[42]
5	thin film	sol-gel	[43]
6	thin film	thermal evaporation	[44]
7	thin film	chemical vapor deposition (CVD)	[45]
8	nanorods	electrophoretic deposition (EPD)	[46]
9	nanowires	hydrothermal	[21]
10	nanostructured film	inkjet printing	[47]
11	nanoparticle film	spray coating	[48]

Electrophoretic deposition was applied in coating hydro-thermally synthesized crystalline WO$_3$ nanorods for EC application by Lee *et al*. [46]. The WO$_3$ nanorods exhibited a fast switching time of 28.8/4.5 s for coloring/bleaching due to the porous nature of the oxide layer (Figure 4(b)). The porous oxide layer allows the electrolyte to penetrate and hence shortens the ionic diffusion length. Furthermore, the high surface area has provided large amount of reaction sites for the Li$^+$ to improve across the oxide-electrolyte interface. In order to improve the EC performance of WO$_3$, the researchers have further increased its specific surface area. WO$_3$ nanowires and nanotrees have been reported in recent years. Hexagonal structured WO$_3$ films with tree-like morphology were synthesized on tungsten foils by Zhang *et al*. [49]. Each nanotree was composed of several (six) nanosheet-shaped "branches". Due to the large tunnels of hexagonal structure and highly porous surface morphology, a switching time of 12.8/8 s for coloring/bleaching (Figure 4(d)) and a CE value of 43.6 cm^2/C were achieved thermal treated (400 °C/2 h) WO$_3$ nanotree. Zhang *et al*. [20] further investigated the WO$_3$ nanowire array film. A hexagonal WO$_3$ nanowire array was obtained using a template-free hydrothermal method by adding ammonium sulfate as a capping agent. The WO$_3$ nanowires were woven together at the surface of the film, forming well-aligned arrays at the bottom part and a porous surface morphology. A switching speed of 7.6/4.2 s for coloring/bleaching (Figure 4(f)) and a CE value of 102.8 cm^2/C were achieved for the WO$_3$ nanowire array film, which showed better EC performance than nanosheets [50], nanorods [46] and nanotrees [49]. The results above suggest that the enhanced EC performance of WO$_3$ nanostructure film is due to the large active surface of a highly porous structure, good contact between the film and the substrate, and large tunnels in the hexagonal WO$_3$.

3.1.2   Metal doping

Doping metal ions with lower oxidizing capacity than host materials are expected to improve the coloration efficiency, reaction kinetics as well as optical modulation. Tungsten oxide with metal doping can have properties that are
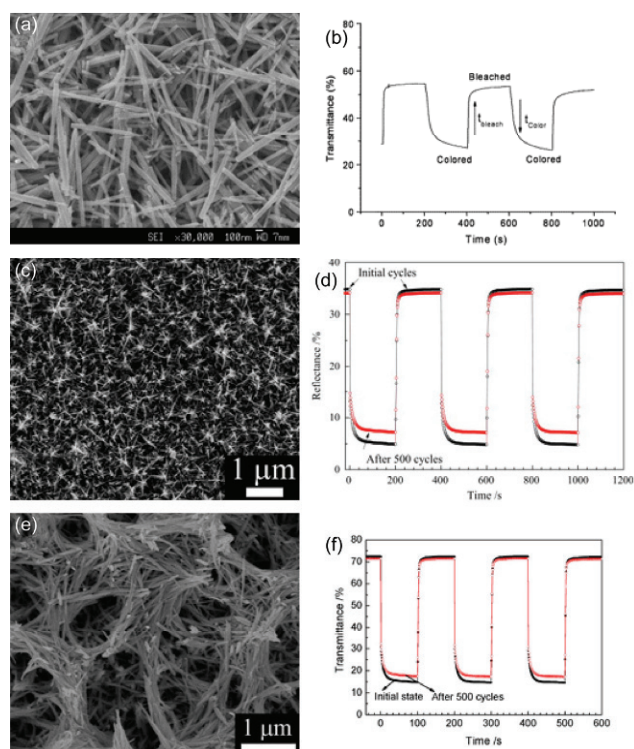

Figure 4   (a) Scanning electron microscope (SEM) image of nanorods; (b) *in situ* transmittance curves at 632.8 nm of nanorods [46]; (c) SEM image of nanotrees; (d) *in situ* reflectance curves at 500 nm of nanotrees [49]; (e) SEM image of nanowires; (f) *in situ* transmittance curves at 633 nm of nanowires [20] (color online).

superior, in one way or another, to those of the pure oxide. Usually, researches on metal doping have been performed with Li, Ti, Mo, Ni, Ru, V, Sn and Ta [8].

There has been great interest in Ti-doped WO$_3$ thin films because Ti addition stabilizes a highly disordered structure, which leads to enhanced durability under electrochemical cycling [8]. Granqvist *et al*. [51] recently discussed the beneficial effects of Ti addition. They prepared W-Ti oxide films with various compositions by reactive dc magnetron sputtering. Figure 5(a, b) shows cyclic voltammograms for W oxide films in two ranges: 2.0–4.0 and 1.7–4.0 V vs.
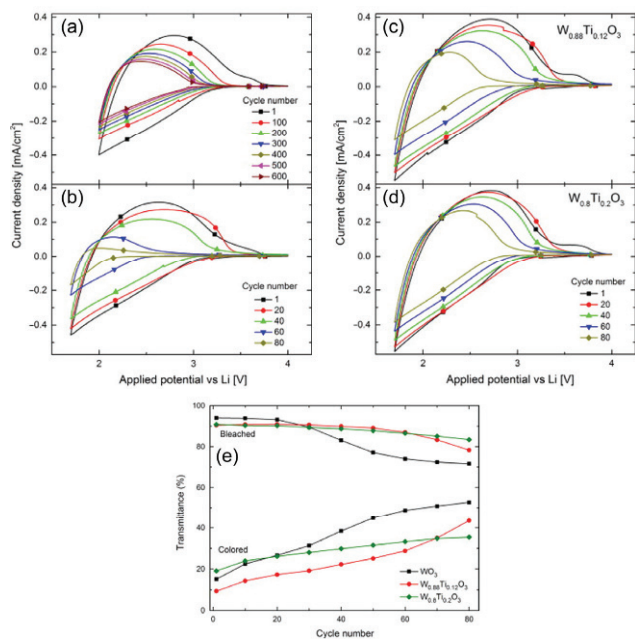
Figure 5 (a, b) Cyclic voltammograms for pure W films. Data were taken after the indicated numbers of cycles and for voltage sweep ranges being 2.0–4.0 V vs. Li (a) and 1.7–4.0 V vs. Li (b). (c, d) Cyclic voltammograms for W-Ti oxide films of the shown compositions. Data were taken after the indicated numbers of cycles and for the sweep range 1.7–4.0 V vs. Li. (e) Evolution of maximum and minimum transmittance at 550 nm for W oxide and W-Ti oxide films of the shown compositions. Data were taken after the indicated numbers of cycles and for the sweep range 1.7–4.0 V vs. Li. The electrolyte was 1 M Li-PC [51] (color online).

Li^+/Li. A gradual decline takes place during 80 CV cycles for the larger voltage interval whereas relative stability is found for the smaller range. As shown in Figure 5(c, d), this degradation is much less significant in thin films of $W_{0.88}Ti_{0.12}O_3$ and is even smaller for $W_{0.8}Ti_{0.2}O_3$. Figure 5(e) shows maximum and minimum monochromatic transmittance at $\lambda=550$ nm, denoted by T_b and T_c, respectively. Corresponding to the CV data, it is apparent that the addition of Ti significantly promotes the cycling performance. Mo oxide is similar in many ways to W oxide, such as crystalline phase. Hence, there are many studies about Mo-W oxide films. Mo-doped WO_3 nanowire arrays were rationally fabricated by a sulfate-assisted hydrothermal method by Zhou *et al.* [52]. Compared to pure WO_3, the optimized Mo-doped WO_3 nanowire arrays exhibited improved EC properties with fast switching speed (3.2/2.6 s for coloring/ bleaching), significant optical modulation (56.7% at 750 nm, 83.0% at 1600 nm and 48.5% at 10 μm), high coloration efficiency (123.5 cm²/C) and excellent cycling stability. Faughan *et al.* [53] reported that the high coloration efficiencies were expected as a result of enhanced electron intervalent transfer between Mo^{5+} and W^{6+}, besides Mo^{5+} to Mo^{6+} and W^{5+} to W^{6+}. The enhanced EC behavior was attributed to an increase in diffusion coefficient of H^+ or Li^+ ion in the films.

3.1.3 Nanostructure composites

Single EC materials still have disadvantages, such as limited colors, slow switching speed, poor cycle stability, due to the low conductivity and large fluctuations in volume during cycling. To alleviate the mechanical strain/stress and improve the electrical conductivity of these materials, an approach of creating a nanocomposite, such as core/shell nanowires has been proven as an effective way.

Recently, graphene has been widely used in lithium-ion batteries, so as electrochromism. WO_3 and reduced graphene oxide (WO_3/rGO) nanocomposites were prepared by a one-step facile electrochemical deposition in an aqueous electrolyte containing tungsten species and graphene oxide by Lee *et al.* [54]. The WO_3/rGO film shows significant improved EC properties, such as shorter switching time (6.8/9.1 s for coloring/bleaching), longer cycle life (85% after 1000 cycles) and larger coloration efficiency (96.1 cm²/C at 632.8 nm), due to the synergistic incorporation of rGO into WO_3. Synthesis of TiO_2 nanotube, nanorod or nanowire structures has also received extensive attention because these structures offer direct electrical pathways for electrons and can increase the electron transport rate. Wang *et al.* [37] fabricated WO_3 nanoparticles loaded in TiO_2 nanotube arrays by a chemical bath deposition (CBD) method in combination with a pyrolysis process. The formation of WO_3/TiO_2 junction achieved the enhanced EC properties of longer lifetime, higher contrast ratio (bleaching time/coloration time) and improved tailored EC behavior. The TiO_2/WO_3 core/shell nanorod arrays were prepared by the combination of hydrothermal and electro-deposition method by Cai *et al.* [55]. In particular, a significant optical modulation (57.2% at 750 nm, 70.3% at 1800 nm and 38.4% at 10 μm), fast switching speed (2.4/1.6 s), high coloration efficiency (67.5 cm²/C at 750 nm) and excellent cycling performance (65.1% after 10000 cycles) are mainly attributed to the core/shell structure and the porous space among the nanorod array.

3.2 Nickel oxide

The most commonly used anodic oxide-based EC materials are Ni and Ir oxide. They can both change from a transparent state to a neutral colored one upon extraction of protons or insertion of OH^- ions [38]. Ir is limited to use due to its high cost and limited supply. Hence, Ni oxide has been studied extensively because of its high optical modulation, fast switching speed, good cyclic stability, memory effect and low cost. Furthermore, NiO can also be ion storage films in the standard EC device, which have the color overlay or complementary effect. The common approaches of fabricating NiO films are listed in Table 2.

It is widely accepted that the EC performance of NiO is attributed to the injection/extraction of electrons and cations [49], which strongly depend on the diffusion length of ions and the appropriate surface area. However, there are still

Table 2   General approaches of fabricating NiO films

Number	Morphology	Method	Reference
1	thin film	sputtering	[56]
2	octahedral-like grains	chemical vapor deposition (CVD)	[57]
3	thin film	spray pyrolysis	[58]
4	thin film	pulsed laser deposition (PLD)	[59]
5	porous thin film	chemical bath deposition (CBD)	[60]
6	thin film	sol-gel	[61]
7	nanostructure thin film	electro-deposition	[29]
8	micro/nanoflowers	hydrothermal	[62]

difficulties in commercial applications of NiO as promising EC materials due to its slow switching speed, low color contrast and poor cycling durability. Hence, it is important to design a material with nanostructure to obtain fast insertion kinetics and enhanced durability. Below we summarize some strategies to improve the EC performance of NiO.

3.2.1   Nanostructures

To date, a variety of NiO nanostructures including nanorods, nanosheets, and nanospheres have been fabricated (Figure 6). A structure with large surface area could both increase the contact area between the electrode and the electrolyte and reduce the diffusion path of ions, which will

Figure 6   (a) SEM images and (b) transmittance spectra of the NiO nanoparticles film with seed layer on the ITO glass [63]; (c) SEM images and (d) transmittance spectra of 1D NiO nanorods [64]; (e) SEM images and (f) transmittance spectra of NiO nanoflakes [60] (color online).

maintain better structure stability that may lead to superior EC performances, such as fast switching time and excellent cyclic stability.

Recently, Lee *et al*. [63] reported that uniform NiO nanoparticle were successfully synthesized, which showed a large optical modulation (63.6% at 550 nm), high coloration efficiency (42.8 cm^2/C at 550 nm) and good cycling stability, which is attributed to the uniform nanoparticles morphology and stable chemical bonding between the NiO nanoparticle and substrates. There are a few reports on the EC properties of one-dimensional (1D) nanorods. Patil *et al*. [64] synthesized 1D NiO nanorods via the hot-filament metal-oxide vapor deposition technique. In comparison with the surface area of the film, the array increased the effective area by 21 times. 1D NiO nanorods showed large diffusion coefficient ($\sim$6.33$\times$10^{-8} cm^2/s), as well as good coloration efficiency (43.3 cm^2/C), large optical transmittance difference (60%), high optical density (1.06) and very fast coloration/bleaching times (1.55/1.22 s) at 630 nm. NiO nanosheets fabricated by CBD have also been studied by researchers. Xia *et al*. [60] reported that highly porous NiO nanoflake film annealed at 300 °C showed a good memory effect and a noticeable EC performance with optical modulation up to 82% and high CE of 42 cm^2/C at 550 nm. The annealed NiO film also showed good reaction kinetics with fast switching speed (8/10 s for coloration/bleaching) due to its highly porous structure. Nanostructures are proven to be a path way to improve the EC performance of materials.

3.2.2   Metal doping

Pure NiO films show poor performance when cycled in electrolytes, especially poor stability and low charge capacity mismatching with WO$_3$. It is found that doping of other elements (such as Li, Mg, Al, Ti, Co) to NiO films could enhance their optical properties and cycle stability.

To our knowledge, NiO and CoO have a similar cubic structure and low lattice mismatch (2.1%), which is suitable to substitutional doping. Moreover, doping Co without causing much lattice strain is possible due to the similar ion radius of Ni and Co. Co-doped NiO thin films by CBD were fabricated by Zhang *et al*. [65]. Co doping significantly affects the growth of NiO film during the CBD process (Figure 7(a–e)). The 1% Co-doped NiO nanoflake array exhibited
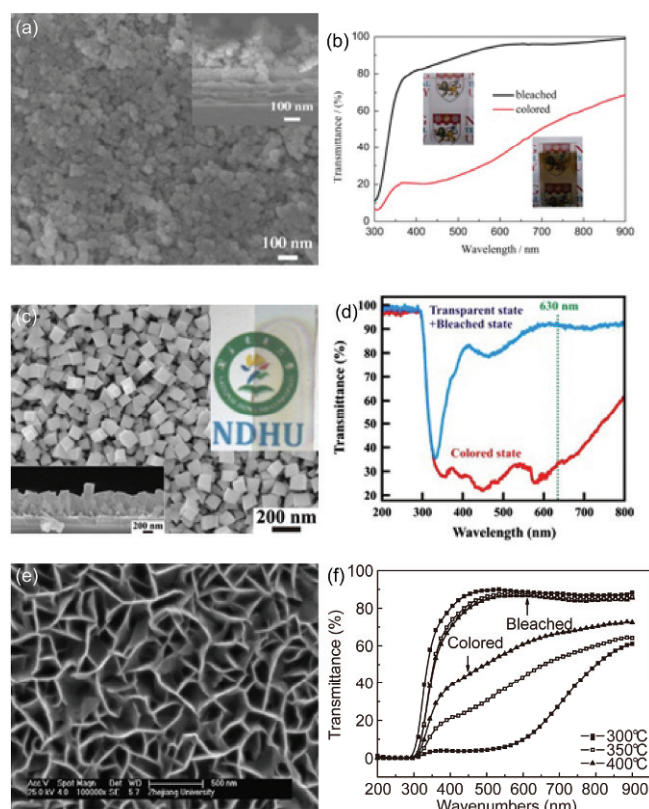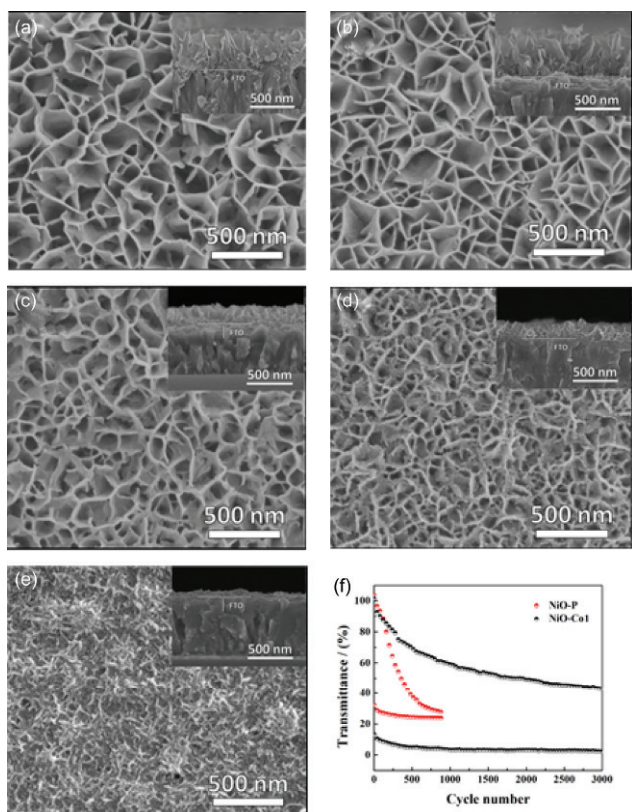
Figure 7 (a–e) SEM images of the films. (a) Pure NiO; (b) NiO-Co0.3; (c) NiO-Co0.5; (d) NiO-Co1; (e) NiO-Co3 (cross-sectional view is presented in the inset). (f) Durability tests of NiO and NiO-Co1 nanoflake array films for 3000 cycles at 550 nm [65] (color online).

outstanding EC performance, including large transmittance modulation (88.3%), high coloration efficiency (47.7 cm^2/C), fast switching speed (3.4/5.4 s for coloration/ bleaching) and excellent cycling durability (54.0% after 3000 cycles) at 550 nm (Figure 7(f)). The enhanced EC performance can be attributed to the synergetic effect contribution from low crystallization, oblique nanoflake array configuration and improved p-type conductivity by appropriate Co doping. Li addition to NiO films displays enhanced EC properties and stability due to the increase of Li$^+$ ion paths when cycled in Li$^+$-based electrolyte. Lately, co-doped NiO films, such as Li-Al-NiO, Li-Zr-NiO and Li-W-NiO, have been studied by researchers, which showed superior EC performance to the traditional mono-doped NiO films [61]. Li-Ti co-doped NiO films prepared by Zhou *et al.* [61], which possessed excellent optical properties and cycle stability (Figure 8(b)). This is due to the combination effect of Li and Ti ions on NiO crystal structure, in which Li$^+$ and Ti^{4+} ions substitute the Ni^{2+} sites, increases the lattice defect and reduce the number of (111) plane. In addition, Li and Ti dopants will modulate the radio of Ni^{2+}/Ni^{3+} and the compositions of the films, resulting in larger transmittance variation in the Li-Ti co-doped NiO films. EC devices assembled with poly(3,4-(2,2-dimethylpropylenedioxy) thiophene) and Li-Ti-NiO films exhibited rapid color change

within 1 s, excellent optical variation for about 56% at 580 nm and high stability up to 1000000 cycles (Figure 8(c–e)).

3.2.3   Nanostructure composites

Aligned TiO$_2$ nanorods have high chemical stability in KOH electrolyte and can be easily synthesized by hydrothermal, which can be used as core for core/shell structure. Cai *et al.* [66] reported that a TiO$_2$/NiO core/shell nanorod array was prepared by a combination of hydrothermal and CBD. This TiO$_2$/NiO core/shell nanorod arrays exhibited larger optical modulation (83%), higher coloration efficiency (60.6 cm^2/C) and better cycling performance (Figure 9(a, b)). The enhanced EC performance is attributed to synergetic contribution from the single crystalline TiO$_2$ nanorod core and the ultrathin NiO nanflake. The TiO$_2$ nanorods can also reduce the refractive index and improve optical transparency, which will be useful to electrochromism. Additionally, the n-type TiO$_2$ core/p-type NiO shell heterostructure can show its advantages, such as improving the separation of electron and proton by the electric junction field, favoring the interfacial charge and enhancing the reaction reversibility and electrochemical activity. Graphene, a two dimensional (2D) crystal that is stable under ambient conditions, is now well used in many research areas due to
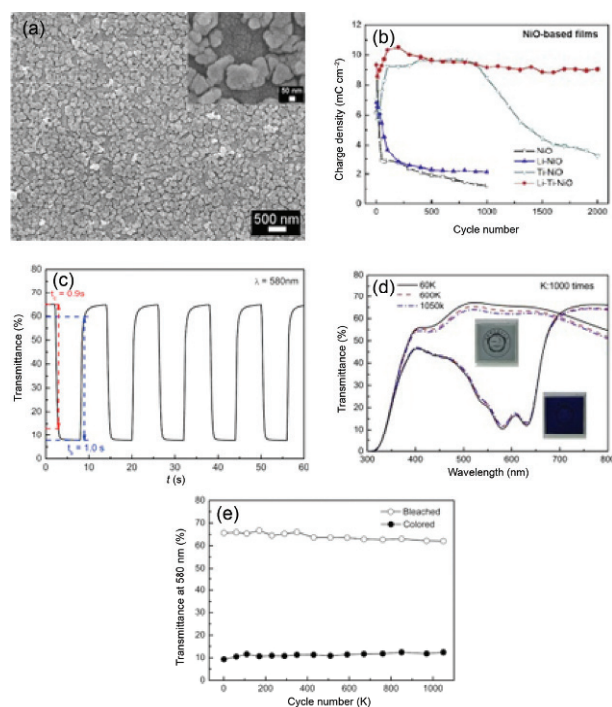

Figure 8 (a) Field emission scanning electron microscope (FESEM) image of Li-Ti-NiO films (high magnification images presented in right top corner inset); (b) charge density variation curves vs. cycle number of NiO-based films tested by chronocoulommetry cycles (±1.5 V, 30 s), EC properties of the PProDOT-Me$_2$/1 M LiClO$_4$ in PC/Li-Ti-NiO device; (c) cyclic light transmittance data for the device measured at 580 nm (±1.5 V, 6 s); (d) optical spectra for device in bleached and colored state (±1.5 V, 2 s); (e) transmittance in bleached and colored state measured at 580 nm as a function of cycle numbers [61] (color online).
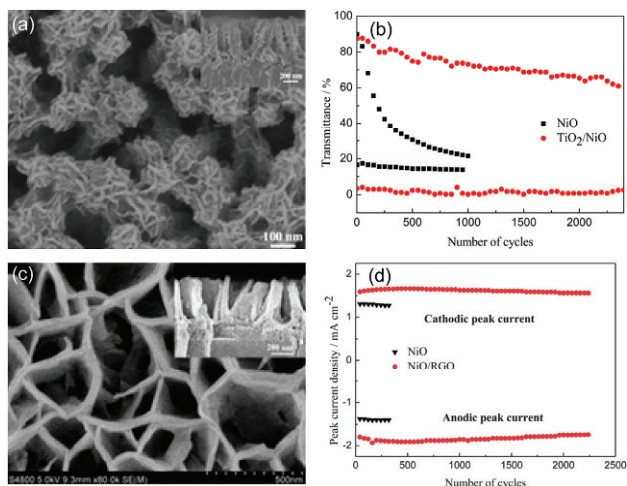
Figure 9 (a) SEM images of TiO$_2$/NiO core/shell nanorod array; (b) durability tests of NiO and TiO$_2$/NiO core/shell nanorod array for 2400 cycles at 550 nm [66]; (c) SEM images of NiO/RGO hybrid film; (d) peak current evolution of porous NiO/RGO hybrid and NiO film during the step chronoamperometric cycles [67] (color online).
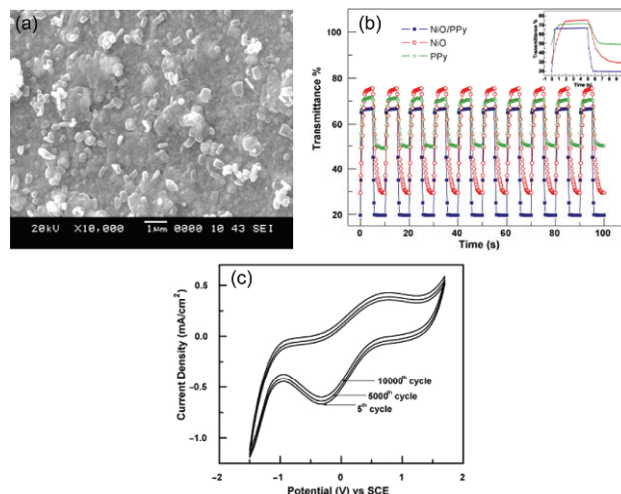

Figure 10 (a) SEM image of NiO/PPy sample; (b) variation of transmittance for NiO, PPy and NiO/PPy as a function of time for the first ten switching cycles between −1.2 and 2.2 V for NiO and −1.5 and 1.5 V vs. SCE for PPy and NiO/PPy; (c) overplay of CVs for NiO/PPy sample after 5 and 10000 cycles. The electrolyte was 1 M LiClO$_4$/PC (color online).

its high carrier mobility, great mechanical strength, and large specific surface area. A porous NiO/rGO hybrid film was fabricated by Cai *et al*. [67] in 2012. The porous hybrid film showed high coloration efficiency (76 cm^2/C), fast switching speed (7.2/6.7 s) and better cycling performance compared with the porous NiO thin film (Figure 9(c, d)).

In addition, many composite structures by combining organic-inorganic hybrid materials have been studied, which can combine the advantages of both the components and offer special properties through modification of each other. A NiO/PPy film was assembled by Patil *et al*. [68]. The NiO/PPy hybrid film showed rich colors (brown to yellow), high coloration efficiency (358 cm^2/C), fast switching time (0.601/0.395 s for coloration/bleaching) and excellent cycle stability (10000 cycles) (Figure 10).

3.3 Electrolytes

Solid electrolytes will become the future trend of EC device' development. There are two types of solid eletrolytes, a solid inorganic salt or polymers containing occluded salt. In the five-layer "battery-type" design, as discussed in Section 2, the electrolyte must be transparent and with no color change when EC device works.

A solid electrolyte is usually a porous oxide, which can conduct H$^+$ or Li$^+$ by co-deposition, chemical or electrochemical post treatment, or by exposure to humidity. Ta oxide has been extensively studied due to its high transparency in the visible and UV range, low leakage current, high dielectric constant, good ionic conductivity, and good chemical and thermal stability [69]. In particular, the solid electrolyte consisting of the Ta$_2$O$_5$ thin film was fabricated as H$^+$ or Li$^+$-containing film [56,70]. In addition, more other film electrolytes have also been investigated, such as

LiNbO$_3$ [71], ZrO$_2$:H [72], LiBO$_2$-Li$_2$SO$_4$ (known as LiBSO) [73].

Polymer electrolytes, including solid polymer electrolytes, gel polymer electrolytes and hybrid polymers, have been used in EC devices. Polymer electrolytes for EC devices should be characterized by an ionic conductivity of 10^{-4} S/cm and cycle stability. Zhang *et al*. [74] reported an all-solid-state EC device based on NiO/WO$_3$ complementary structure with solid polyelectrolyte (Figure 11). The device showed an optical modulation of 55% at 550 nm, a CE value of 87 cm^2/C, fast switching time (10/20 s for coloration/bleaching) and cycling stability (1600 cycles). Polyvinyl alcohol (PVA)-based electrolytes have been extensively used in energy storage, as well as EC devices. An EC device based on PVA and borax, in combination with a viologen and a redox pair has been developed by Alesanco *et al*. [75]. The electrolyte has excellent mechanical strength and transparency. A significant optical contrast (>65% at 550 nm), switching time (<5 s) and cyclability (8000–10000) have been achieved. The viscoelastic fluid character of the electrolyte mixture is convenient to assemble the EC devices, which will be further used in future. In addition, researchers have also studied other polymer electrolytes, such as poly(methylmethacrylate)-based electrolytes [47], gelatin-and agar-based electrolytes [76,77], polymethacrylate hydroxyethylene resins [78], plasma electrolytic oxidation (PEO)- or poly(vinylidene fluoride) (PVDF)-based electrolytes [79].

4 Conclusions and outlook

In summary, we review basic EC device designs, useful oxide materials (tungsten oxide/nickel oxide), solid-state
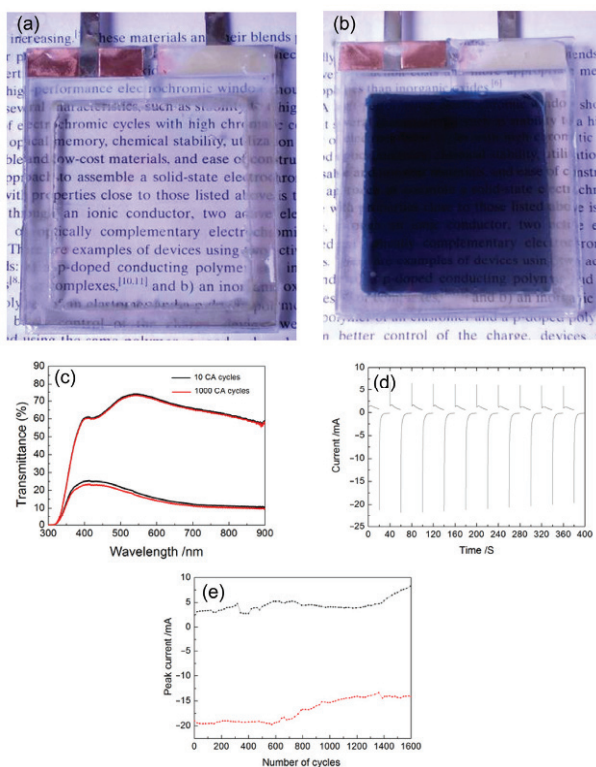
Figure 11 (a, b) Bleached and coloration state of ECD; (c) optical transmittance spectra of ECD of 10th CA cycle and 1000th CA cycle; (d, e) step chronoamperometric (CA) curves of the device: current-time response curve of the device (d), and peak current during the step chronoamperometric cycles (e) [74] (color online).

electrolytes. It is clear that optical modulation, CE value, switching speed, and sometimes stabilities can be significantly improved by nanostructures, metal doping and nanostructure composites due to the enhanced electron and ion transport as well as donor-acceptor interactions. The extent of the donor-acceptor interactions at interface is highly dependent on interfacial area and the nature of the interactions at interface. To boost the performance of ECs, it is crucial to design proper electrode structure, which makes organic and inorganic active phases working together and simultaneously exhibits color change to improve optical modulation in the same voltage window. In addition, solid-state electrolyte is another most significant challenge in EC devices for their further commercial applications. The early studies of polymer electrolytes have provided copious amount of data, which will lead us to go on. Thermal and electrochemical stability of polymer electrolytes will be the major research for us since stability will reflect product safety, recyclability and self-life.

It is necessary to further optimize the synthesis of metal oxide based EC films with controlled morphologies by using nanostructures, composites and doping. And systematic study on the effect of morphology on EC properties is needed. It is also urgent to investigate the formation process of microstructure of EC films and the cations intercalation/

deintercalation mechanisms during electrochemical reactions. Furthermore, the electrolytes used in the devices should have different influence on the EC properties, and therefore should be investigated in detail.

The metal-oxide/conducting polymer hybrids/composites based materials for EC devices are very promising because of the synergic advantages of them, and the drawbacks of single color, low switching speed, poor cyclic stability and low CE can be overcome. However, the microstructure design of the organic/inorganic hybrids/composites remains a challenge for future commercialization.

Ultimately, it is essential to understand the compatibility and joint EC mechanism of EC layer, electrolyte layer, ion-storage layer of the all-solid-state devices with metal-oxide and conducting polymers. The development of state-of-the-art with energy-storage devices or dye-sensitized solar cell will improve the packaging technology of EC devices. Multifunctional films in devices may enable multifunctional EC devices accompanying with supercapacitors or solar cells.

Conflict of interest   The authors declare that they have no conflict of interest.

1   Granqvist CG. *Nat Mater*, 2006, 5: 89–90
2   Granqvist CG. *Adv Mater*, 2003, 15: 1789–1803
3   Granqvist CG. *Sol Energ Mat Sol C*, 2012, 99: 1–13
4   Wen RT, Granqvist CG, Niklasson GA. *Nat Mater*, 2015, 14: 996–1001
5   Xia XH, Chao DL, Qi XY, Xiong QQ, Zhang YQ, Tu JP, Zhang H, Fan HJ. *Nano Lett*, 2013, 13: 4562–4568
6   Granqvist CG. *Handbook of Inorganic Electrochromic Materials*. Amsterdam: Elsevier, 1995: 1–15
7   Cai GF, Tu JP, Zhou D, Wang XL, Gu CD. *Sol Energ Mat Sol C*, 2014, 124: 103–110
8   Granqvist CG. *Thin Solid Films*, 2014, 564: 1–38
9   Platt JR. *J Chem Phys*, 1961, 34: 862–863
10 Deb SK. *Appl Optics*, 1969, 8: 192–195
11 Deb SK. *Philos Mag*, 1973, 27: 801–822
12 Deb SK. *Sol Energ Mat Sol C*, 1995, 39: 191–201
13 Schoot CJ, Ponjee JJ, van Dam HT, van Doorn RA, Bolwijn PT. *Appl Phys Lett*, 1973, 23: 64–65
14 Monk P, Mortimer R, Rosseinsky D. *Electrochromism: Fundamentals and Applications*. Veinheim: Wiley-VCH, 1999: 42–47
15 Mortimer RJ. *Electrochim Acta*, 1999, 44: 2971–2981
16 Granqvist CG. *Electrochim Acta*, 1999, 44: 3005–3015
17 Granqvist CG. *Sol Energ Mat Sol C*, 2000, 60: 201–262
18 Green M. *Chem Ind*, 1996: 641–644
19 Rosseinsky DR, Mortimer RJ. *Adv Mater*, 2001, 13: 783–793
20 Zhang J, Tu JP, Xia XH, Wang XL, Gu CD. *J Mater Chem*, 2011, 21: 5492–5498
21 Zhou D, Xie D, Shi F, Wang DH, Ge X, Xia XH, Wang XL, Gu CD, Tu JP. *J Colloid Interf Sci*, 2015, 460: 200–208
22 Cai GF, Tu JP, Zhou D, Li L, Zhang JH, Wang XL, Gu CD. *CrystEngComm*, 2014, 16: 6866–6872
23 Kharraz M, Azens A, Kullman L, Granqvist CG. *Thin Solid Films*, 1997, 295: 117–121

24 Liu Y, Lv Y, Tang ZB, He LG, Liu XY. *Electrochim Acta*, 2016, 189: 184–189
25 Wang CM, Lin SY. *J Solid State Electr*, 2006, 10: 255–259
26 Nang Dinh N, Minh Quyen N, Chung DN, Zikova M, Truong VV. *Sol Energ Mat Sol C*, 2011, 95: 618–623
27 Patil RA, Devan RS, Liou Y, Ma YR. *Sol Energ Mat Sol C*, 2016, 147: 240–245
28 Xia XH, Tu JP, Zhang J, Wang XL, Zhang WK, Huang H. *Electrochim Acta*, 2008, 53: 5721–5724
29 Cai GF, Tu JP, Gu CD, Zhang JH, Chen J, Zhou D, Shi SJ, Wang XL. *J Mater Chem A*, 2013, 1: 4286–4292
30 Zhang JH, Tu JP, Zhou D, Tang H, Li L, Wang XL, Gu CD. *J Mater Chem C*, 2014, 2: 10409–10417
31 Xia XH, Tu JP, Zhang J, Xiang JY, Wang XL, Zhao XB. *Sol Energ Mat Sol C*, 2010, 94: 386–389
32 Xia XH, Tu JP, Zhang J, Xiang JY, Wang XL, Zhao XB. *ACS Appl Mater Interfaces*, 2010, 2: 186–192
33 Goldner RB, Haas TE, Arntz FO, Slaven S, Wong KK, Wilkens B, Shepard C, Lanford W. *Appl Phys Lett*, 1993, 62: 1699–1701
34 Gratzel M. *Nature*, 2001, 409: 575–576
35 Santos L, Wojcik P, Pinto JV, Elangovan E, Viegas J, Pereira L, Martins R, Fortunato E. *Adv Electron Mater*, 2015, 1: 1400002
36 Lee SH, Deshpande R, Parilla PA, Jones KM, To B, Mahan AH, Dillon AC. *Adv Mater*, 2006, 18: 763–766
37 Song YY, Gao ZD, Wang JH, Xia XH, Lynch R. *Adv Funct Mater*, 2011, 21: 1941–1946
38 Cai GF, Tu JP, Zhou D, Zhang JH, Wang XL, Gu CD. *Sol Energ Mat Sol C*, 2014, 122: 51–58
39 Yamada Y, Tabata K, Yashima T. *Sol Energ Mat Sol C*, 2007, 91: 29–37
40 Wang LY, Yuan L, Wu XF, Wu J, Hou CM, Feng SH. *RSC Adv*, 2014, 4: 47670–47676
41 Pauporté T. *J Electrochem Soc*, 2002, 149: C539–C545
42 Zhang J, Wang XL, Xia XH, Gu CD, Zhao ZJ, Tu JP. *Electrochim Acta*, 2010, 55: 6953–6958
43 Zhao BW, Zhang X, Dong GB, Wang H, Yan H. *Ionics*, 2015, 21: 2879–2887
44 Patel KJ, Panchal CJ, Desai MS, Mehta PK. *Mater Chem Phys*, 2010, 124: 884–890
45 Dimitrova Z, Gogova D. *Mater Res Bull*, 2005, 40: 333–340
46 Khoo E, Lee PS, Ma J. *J Eur Ceram Soc*, 2010, 30: 1139–1144
47 Cai GF, Darmawan P, Cui MQ, Chen JW, Wang X, Eh ALS, Magdassi S, Lee PS. *Nanoscale*, 2016. 8: 348–357
48 Li HZ, Chen JW, Cui MQ, Cai GF, Eh ALS, Lee PS, Wang HZ, Zhang QH, Li YG. *J Mater Chem C*, 2016, 4: 33–38
49 Zhang J, Wang XL, Xia XH, Gu CD, Tu JP. *Sol Energ Mat Sol C*, 2011, 95: 2107–2112
50 Xiao W, Liu WT, Mao XH, Zhu H, Wang DH. *J Mater Chem A*, 2013, 1: 1261–1269
51 Arvizu MA, Triana CA, Stefanov BI, Granqvist CG, Niklasson GA. *Sol Energ Mat Sol C*, 2014, 125: 184–189
52 Zhou D, Shi F, Xie D, Wang DH, Xia XH, Wang XL, Gu CD, Tu JP. *J Colloid Interf Sci*, 2016, 465: 112–120
53 Faughnan BW, Crandall RS. *Appl Phys Lett*, 1977, 31: 834–836
54 Fu C, Foo C, Lee PS. *Electrochim Acta*, 2014, 117: 139–144
55 Cai GF, Zhou D, Xiong QQ, Zhang JH, Wang XL, Gu CD, Tu JP. *Sol Energ Mat Sol C*, 2013, 117: 231–238
56 Song XW, Dong GB, Gao FY, Xiao Y, Liu QR, Diao XG. *Vacuum*, 2015, 111: 48–54
57 Sialvi MZ, Mortimer RJ, Wilcox GD, Teridi AM, Varley TS, Wijayantha KGU, Kirk CA. *ACS Appl Mater Interfaces*, 2013, 5: 5675–5682
58 Denayer J, Bister G, Simonis P, Colson P, Maho A, Aubry P, Vertruyen B, Henrist C, Lardot V, Cambier F, Cloots R. *Appl Surf Sci*, 2014, 321: 61–69
59 Moulki H, Park DH, Min BK, Kwon H, Hwang SJ, Choy JH, Toupance T, Campet G, Rougier A. *Electrochim Acta*, 2012, 74: 46–52
60 Xia XH, Tu JP, Zhang J, Wang XL, Zhang WK, Huang H. *Sol Energ Mat Sol C*, 2008, 92: 628–633
61 Zhou JL, Luo G, Wei YX, Zheng JM, Xu CY. *Electrochim Acta*, 2015, 186: 182–191
62 Zhao CC, Du FL, Wang JM. *RSC Adv*, 2015, 5: 38706–38711
63 Cai GF, Wang X, Cui MQ, Darmawan P, Wang JX, Eh ALS, Lee PS. *Nano Energy*, 2015, 12: 258–267
64 Patil RA, Devan RS, Lin JH, Ma YR, Patil PS, Liou Y. *Sol Energ Mat Sol C*, 2013, 112: 91–96
65 Zhang JH, Cai GF, Zhou D, Tang H, Wang XL, Gu CD, Tu JP. *J Mater Chem C*, 2014, 2: 7013–7021
66 Cai GF, Tu JP, Zhou D, Li L, Zhang JH, Wang XL, Gu CD. *J Phys Chem C*, 2014, 118: 6690–6696
67 Cai GF, Tu JP, Zhang J, Mai YJ, Lu Y, Gu CD, Wang XL. *Nanoscale*, 2012, 4: 5724–5730
68 Sonavane AC, Inamdar AI, Dalavi DS, Deshmukh HP, Patil PS. *Electrochim Acta*, 2010, 55: 2344–2351
69 Wang SC, Liu KY, Huang JL. *Thin Solid Films*, 2011, 520: 1454–1459
70 Tajima K, Yamada Y, Bao S, Okada M, Yoshimura K. *J Electrochem Soc*, 2010, 157: J92–J96
71 Zhang XP, Zhang HK, Li Q, Luo HL. *IEEE Electr Device Lett*, 2000, 21: 215–217
72 Zhou YL, Diao XG, Dong GB, Wu ZH, Dong DM, Wang M. *Ionics*, 2016, 22: 25–32
73 Yang HG, Wang C, Zhu KG, Diao XG, Wang HY, Cui Y, Wang TM. *Chinese Phys Lett*, 2008, 25: 740
74 Zhang J, Tu JP, Xia XH, Qiao Y, Lu Y. *Sol Energ Mat Sol C*, 2009, 93: 1840–1845
75 Alesanco Y, Palenzuela J, Viñuales A, Cabañero G, Grande HJ, Odriozola I. *ChemElectroChem*, 2015, 2: 218–223
76 Ponez L, Sentanin FC, Majid SR, Arof AK, Pawlicka A. *Mol Cryst Liq Cryst*, 2012, 554: 239–251
77 Raphael E, Avellaneda CO, Aegerter MA, Silva MM, Pawlicka A. *Mol Cryst Liq Cryst*, 2012, 554: 264–272
78 Gonçalves A, Costa C, Pereira S, Correia N, Silva M, Barbosa P, Rodrigues L, Henriques I, Martins R, Fortunato E. *Polym Advan Technol*, 2012, 23: 791–795
79 Thakur VK, Ding GQ, Ma J, Lee PS, Lu XH. *Adv Mater*, 2012, 24: 4071–4096